THE ASTROPHYSICAL JOURNAL, 494:523–534, 1998 February 20

EGRET OBSERVATIONS OF THE EXTRAGALACTIC GAMMA-RAY EMISSION

P. SREEKUMAR,[1,2] D. L. BERTSCH,[1] B. L. DINGUS,[3] J. A. ESPOSITO,[1,2] C. E. FICHTEL,[1] R. C. HARTMAN,[1]
S. D. HUNTER,[1] G. KANBACH,[4] D. A. KNIFFEN,[5] Y. C. LIN,[6] H. A. MAYER-HASSELWANDER,[4]
P. F. MICHELSON,[6] C. VON MONTIGNY,[7] A. MÜCKE,[4] R. MUKHERJEE,[8] P. L. NOLAN,[6]
M. POHL,[9] O. REIMER,[4] E. SCHNEID,[10] J. G. STACY,[11] F. W. STECKER,[1]
D. J. THOMPSON,[1] AND T. D. WILLIS[6]

Received 1997 April 17; accepted 1997 September 29

ABSTRACT

The all-sky survey in high-energy gamma rays ($E > 30$ MeV) carried out by EGRET aboard the *Compton Gamma Ray Observatory* provides a unique opportunity to examine in detail the diffuse gamma-ray emission. The observed diffuse emission has a Galactic component arising from cosmic-ray interactions with the local interstellar gas and radiation, as well as an almost uniformly distributed component that is generally believed to originate outside the Galaxy. Through a careful study and removal of the Galactic diffuse emission, the flux, spectrum, and uniformity of the extragalactic emission are deduced. The analysis indicates that the extragalactic emission is well described by a power-law photon spectrum with an index of $-(2.10 \pm 0.03)$ in the 30 MeV to 100 GeV energy range. No large-scale spatial anisotropy or changes in the energy spectrum are observed in the deduced extragalactic emission. The most likely explanation for the origin of this extragalactic high-energy gamma-ray emission is that it arises primarily from unresolved gamma-ray–emitting blazars.

Subject headings: diffuse radiation — gamma rays: observations — surveys

1. INTRODUCTION

Observations at all wavelengths from radio to gamma rays have shown the presence of a diffuse background emission that appears to emanate from beyond our Galaxy. It is generally believed that these extragalactic photons have different origins, which may be broadly thought of as arising from truly diffuse processes or from the contributions of a large number of unresolved point sources. The X-ray background (below 100 keV) is generally understood to arise primarily from the integrated emission of unresolved active galactic nuclei (AGNs) (Leiter & Boldt 1992; Comastri et al. 1995; Zdziarski et al. 1995) such as Seyfert galaxies with redshifts ranging up to 5. In the low-energy gamma-ray regime (0.5–10 MeV) the measurement of an extragalactic component is made difficult by the presence of significant instrumental background, nuclear line emission, and emission from strong sources. Recent results from the COMPTEL instrument (Kappadath et al. 1996) on the *Compton Gamma Ray Observatory* (*CGRO*) and the *Solar Maximum Mission* (*SMM*) (Watanabe et al. 1997), indicate the presence of an extragalactic component significantly lower than previous measurements. At higher energies (>30 MeV), the *OSO 3* satellite provided the first evidence for gamma-ray emission from our Galaxy (Kraushaar et al. 1972). This was followed by observations by the *SAS 2* satellite (Fichtel et al. 1975), which provided clear evidence for a strong correlation of the observed diffuse emission with the expected gamma-ray emission from cosmic-ray, matter, and photon interactions. In addition, the *SAS 2* results also indicated, for the first time, the presence of a residual, apparently isotropic emission that was interpreted as not being associated with the Galaxy and hence of extragalactic origin (Fichtel et al. 1977; Fichtel, Simpson, & Thompson 1978). The *SAS 2* telescope had been carefully designed and tested to have a very low instrumental background (Derdeyn et al. 1972) and had been launched into a near equatorial orbit to minimize the effects of trapped radiation. This was necessary to carry out observations of this diffuse radiation. In the final analysis of the *SAS 2* data (Thompson & Fichtel 1982), the integral intensity above 100 MeV was determined to be $(1.3 \pm 0.5) \times 10^{-5}$ photons cm^{-2} s^{-1} sr^{-1} and the slope of the spectrum to be $-2.35^{+0.4}_{-0.3}$. Detailed measurements of the isotropy were not possible, but the *SAS 2* results did show that the center-to-anticenter ratio for the radiation within $20° < |b| < 40°$ was 1.10 ± 0.19 and the ratio of the intensity perpendicular to the plane to that in the $20° < |b| < 40°$ region was 0.87 ± 0.09 (Fichtel et al. 1978). Thus, these early results did suggest that there was no evidence for significant large-scale anisotropy in the extragalactic gamma-ray emission.

With more than an order of magnitude increase in sensitivity over previous experiments, a low instrumental background, and a low-altitude orbit, EGRET has provided an opportunity to study the spectrum and distribution of the extragalactic emission in greater detail than was possible in the past. The *Compton Gamma Ray Observatory* was launched in 1991 April. A prime objective of EGRET was to carry out the first all-sky survey in high-energy gamma rays (30 MeV $\leq E \leq$ 30 GeV). The most striking feature of the diffuse radiation is the dominant emission from the Galaxy that, fortunately for the study of the extragalactic emission,

[1] NASA/Goddard Space Flight Center, Code 660, Greenbelt, MD 20771.
[2] Universities Space Research Association.
[3] University of Utah, Salt Lake City, UT 84112.
[4] Max-Planck-Institut für extraterrestrische Physik, 8046 Garching bei München, Germany.
[5] Hampden-Sydney College, P. O. Box 862, Hampden-Sydney, VA 23943.
[6] W. W. Hansen Experimental Physics Laboratory, Stanford University, Stanford, CA 94305-4085.
[7] Landessternwarte Heidelberg-Königstuhl, Heidelberg, Germany.
[8] Barnard College, New York, NY 10027.
[9] Danish Space Research Institute.
[10] Northrop Grumman Aerospace Corporation, Mail Stop A01-26, Bethpage, NY 11714.
[11] University of New Hampshire, Durham, NH 03428.

is strongly concentrated along the Galactic plane. The survey also shows the presence of many pointlike sources, some of which have been identified with pulsars, molecular clouds, active galactic nuclei, and a nearby normal galaxy (LMC). About 51 sources have been identified with a class of AGNs called blazars (Thompson et al. 1996; Mattox et al. 1997; Mukherjee et al. 1997) that are, in general, radio-bright AGNs with flat radio spectra, strong optical polarization, superluminal motion (often), and significant time variability at most wavelengths. EGRET observations have shown that for a majority of the gamma-ray luminous blazars, the gamma-ray emission dominates the bolometric luminosity (von Montigny et al. 1995), at least during outbursts.

This paper discusses the findings on the diffuse high-energy gamma-ray emission at high latitudes ($|b| \geq 10°$). A detailed description of the intense Galactic plane emission is provided by Hunter et al. (1997). We discuss the approach used to study the residual, presumably extragalactic high-energy gamma radiation by carefully accounting for the foreground Galactic emission. The spectral and spatial distributions are determined. Possible origins of the extragalactic emission are considered, including the question of whether it is truly diffuse or results from unresolved point-source contributions.

2. OBSERVATIONS

The EGRET instrument is sensitive to gamma rays in the energy range from about 30 MeV to 100 GeV. Gamma rays are detected using a multilevel thin plate spark chamber system using the pair production process. An internal triggering telescope detects the presence of the electron-positron pair with the correct direction of motion and a large NaI(Tl) crystal acts as energy-measuring calorimeter. An anticoincidence dome provides discrimination against the relatively intense charged-particle radiation in space. A detailed description of the instrument is given by Kanbach et al. (1988) and details on the instrument calibration and analysis procedures are available in Thompson et al. (1993), Fichtel et al. (1993), and Esposito et al. (1997). In the wide field-of-view operational mode used for most of the observations discussed here, the effective area of the telescope is about 1000 cm^2 at 100 MeV, rises to 1500 cm^2 around 0.5–1 GeV, and decreases gradually at higher energies to about 700 cm^2 at 10 GeV near the center of the field of view. The effective area is a maximum when the target is on axis, falls to approximately 50% of this value when the angular offset reaches 18°, and has a useful sensitivity to at least 30°. The large field of view of EGRET is important for the study of the diffuse radiation being discussed here.

EGRET observations from 1991 April to 1994 September (phases I, II, and III) are used in the analysis reported here. These were obtained using the full field-of-view mode of the instrument and running the calorimeter in coincidence with spark chamber triggers. Maps of counts, exposure, and intensity are generated in sky coordinates with 0.5×0.5 bins for the individual observations. They are combined to create all-sky maps. Only data from within 30° of the pointing direction of the individual observations, within which the exposure and instrument characteristics are best understood, are used in creating the added maps. The combined exposure map (see Fig. 2 in Thompson et al. 1996) indicates nonuniform sky coverage that needs to be taken into account during the analysis.

3. BACKGROUND CONTRIBUTIONS

Determining the extragalactic diffuse radiation is one of the more difficult measurements, because of the very low intensity of the expected emission and the lack of a spatial or temporal signature to separate the cosmic signal from other radiation. As will be shown the spectrum, is significantly different from the Galactic diffuse radiation. In order to study the extragalactic emission, one must subtract from the observation any instrumental background, the Galactic diffuse emission, and the contribution from resolved point sources.

3.1. *Instrumental Background*

It is essential to demonstrate that the instrumental background is kept well below the level of diffuse emission under study. Hence three separate factors must be considered in the design and implementation of any space-borne high-energy gamma-ray detector used to study the extragalactic diffuse emission: a low cosmic-ray intensity environment for the spacecraft, the detailed instrument design, and its placement on the spacecraft. Only the *SAS 2* and EGRET instruments had a background well below the intensity of the now measured diffuse extragalactic emission. *CGRO* was placed into a standard 28° inclination orbit using a shuttle launch. For the first 6 years after launch, *CGRO* was kept below ~400–450 kilometer altitude to minimize the effects of the trapped radiation. Important features of the instrument design include the directional trigger system, the highly efficient (1 part in 10^6) anticoincidence dome, and the amount and placement of the material above the anticoincidence dome. The typical cosmic-ray flux in orbit that EGRET sees is about 10^4 times the average gamma-ray flux. The high efficiency for rejection of cosmic-ray events by the anticoincidence dome ensures that nearly all cosmic-ray induced events are removed. However, cosmic rays impinging on material above the anticoincidence dome could produce neutral pions via inelastic collisions that decay into gamma rays. Clearly, the material must be kept to a minimum consistent with thermal and light penetration, but it must also be kept very close to the anticoincidence scintillator to maximize the probability that a secondary in any of the very improbable interactions will penetrate and trigger the anticoincidence dome. A new problem arose in the design of EGRET late in its development when, during the repair of the *Solar Maximum Mission* satellite, it was discovered that the space debris had become much more intense than previous estimates. A penetration of the light shield surrounding the anticoincidence dome would cause a small light leak, significantly degrading its performance. Through a special design of the covering material the total amount of matter on the outside of the dome was held on an average to only 20% more than that of *SAS 2* (~0.19 g cm^{-2} compared to ~0.16 g cm^{-2}). In addition, this material was kept close to the anticoincidence dome in order to have the highest probability for a secondary charged particle to enter and trigger the anticoincidence system. Extensive preflight calibration was carried out at the Brookhaven Laboratory to examine the background contribution from the material above the anticoincidence dome. These tests demonstrated that the instrumental background was more than an order of magnitude less than the intensity of the extragalactic diffuse radiation derived from the *SAS 2* data (Thompson et al. 1993). Furthermore, a

steeper spectrum is expected for the cosmic-ray induced instrumental background.

A potential source of contamination is from Earth's albedo gamma rays. These gamma rays arise from cosmic-ray interactions in the Earth's upper atmosphere and are indistinguishable from cosmic gamma rays in the spark chamber. EGRET triggering is disabled during the Earth occultation part of the orbit. As described in Thompson et al. (1993), EGRET carries two 4×4 arrays of scintillator tiles that allow a set of 96 possible subtelescope combinations. As the Earth enters the field of view of any of the direction modes, triggering is disabled for that mode, and thus events with an arrival direction defined by that direction mode are not accepted. However, the albedo gamma-ray flux is quite large and peaks toward the horizon where it is about 10 times more intense than toward the nadir (Thompson, Simpson, & Özel 1981), resulting in the inclusion of a large number of Earth albedo events in the primary data. The elimination of these Earth albedo events is carried out as follows. An energy-dependent cutoff in zenith angle $[\phi_{\rm cutoff}(E)]$ is defined where the zenith angle $[\phi(E)]$ is defined as the angle made by the incoming gamma ray with the direction of the Earth center to spacecraft vector. Events with zenith angles larger than $\phi_{\rm cutoff}(E)$ are rejected, where $\phi_{\rm cutoff}(E) = 110^\circ - \sigma\theta(E)$, where $\theta(E) = 5.^\circ 85\ (E/100\ {\rm MeV})^{-0.534}$ is the calibrated instrument point-spread function (Thompson et al. 1993). In order to sufficiently eliminate the inclusion of albedo events, a σ value of 4.0 is used for the analysis of the extragalactic emission, which is more restrictive than the value 2.5 used for the standard EGRET analysis of point sources. The value of $\phi_{\rm cutoff}(E)$ is further restricted to a minimum value of 80° at low energies to minimize excessive loss of good events and not to exceed a maximum of 105° at high energies. Use of the new values of $\phi_{\rm cutoff}(E)$ also removed some albedo events that appeared to show nonuniform spatial clustering in the summed data (Willis 1996). Since there is only a negligible loss of good events as a result of this tighter restriction in zenith angle, no corrections are applied to the data.

A final check of the contamination of the in-flight data from the charged-particle background is carried out by studying the rigidity dependence of the accepted events. The cutoff rigidity for charged cosmic rays, which varies throughout the orbit, defines the minimum momentum per unit charge necessary to avoid being excluded by the Earth's magnetic field. So regions along the orbit characterized by high magnetic field strengths have a smaller cosmic-ray flux. Figure 1 shows a rigidity plot of the histogram of event rates after imposing all selection criteria for a range of observations. A K-S test using rigidity intervals of less than 0.1 GV yielded negligible probability for the distribution of event rate to be correlated with rigidity, which implies there is no significant charged-particle contribution to the extragalactic emission being discussed here. There is indeed the possibility of high-rigidity (>20 GV) cosmic-ray particles contributing to the background since they are not modulated by the Earth's magnetic field. However, these charged particles have a high probability of producing additional charged particles along with the gamma rays during the interaction with the material ahead of the anticoincidence dome and thus enabling the anticoincidence system to reject the event.

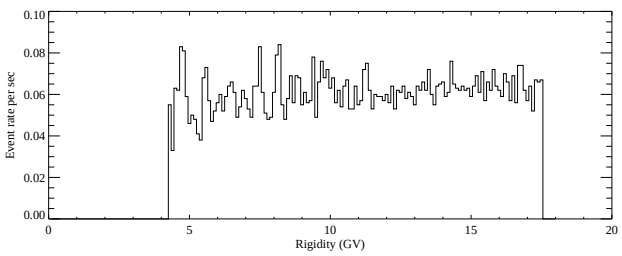

FIG. 1.—Accepted gamma-ray events as a function of geomagnetic rigidity. The absence of a rigidity dependence implies no measurable contamination by charged-particle induced events.

3.2. *Galactic Diffuse Emission*

The Galaxy is a strong source of high-energy gamma rays arising primarily from the interaction of cosmic rays with the interstellar matter and, to a lesser extent, interstellar photons. This emission is strongest within $\pm 60^\circ$ in Galactic longitude and $\pm 10^\circ$ in Galactic latitude, where most of the interstellar gas is present. It falls off rapidly at higher latitudes. The primary processes that produce the observed Galactic diffuse gamma rays are cosmic-ray nucleons interacting with nucleons in the interstellar gas, bremsstrahlung by cosmic-ray electron, and inverse Compton interaction of cosmic-ray electrons with ambient low-energy interstellar photons (Bertsch et al. 1993; Hunter et al. 1997). The possible contribution from unresolved point sources such as pulsars is uncertain with estimates ranging from a few percent to almost 100% depending on the birth properties of pulsars (Bailes & Kniffen 1992). The evidence for a pion "bump" in the Galactic diffuse spectrum (Hunter et al. 1997) implies the unresolved source contribution is well below 50%; however, a contribution $\leq 20\%$ cannot be ruled out at present. No effort is made to incorporate an unresolved source component in the Galactic diffuse calculations used in this study. The electron bremsstrahlung and neutral pion decay processes dominate the diffuse emission, although at higher latitudes the inverse Compton process could contribute up to 30% of the total observed Galactic radiation, particularly in the inner Galaxy. The calculations use deconvolved matter density distribution along with some assumptions about the corresponding cosmic-ray density distribution. Bertsch et al. (1993) and Hunter et al. (1997) discuss the detailed calculation of the diffuse emission from the Galactic plane, including the approach used to derive the Galactic cosmic-ray density distribution. At latitudes $|b| \geq 10^\circ$, the calculation of the Galactic diffuse emission is more straightforward, since the gas distribution along the line of sight is mostly local (within a few hundred parsecs) and the corresponding cosmic-ray spectrum at energies important for gamma-ray production is not expected to be very different from that which is measured locally at Earth, corrected for solar modulation.

The primary inputs necessary to calculate the expected level of diffuse gamma-ray emission in our Galaxy include the distribution of interstellar hydrogen gas (neutral and ionized), low-energy photon distribution (3 K, IR, visible, UV), and the cosmic-ray density, spectrum and composition in the Galaxy along every line of sight. As stated before, the high-latitude ($|b| \geq 10^\circ$) calculation assumes, the spectrum of cosmic rays (electrons and protons) is the same as that measured locally, corrected for solar modulation. The neutral atomic hydrogen distribution is derived from the 21 cm map of Dickey & Lockman (1990), while the molecular

hydrogen distribution is derived indirectly using the strength of $^{12}C^{16}O$ emission at 2.6 mm provided by Dame et al. (1987) [converted into H_2 column density including a normalization factor of 1.5×10^{20} cm^{-2} (K km s^{-1})$^{-1}$; Hunter et al. 1997]. Recent enhancements to the Dame et al. (1987) work by S. Digel (1996, private communication) are included. The ionized interstellar medium is not as well determined. The model of Taylor & Cordes (1993) based on radio pulsar studies is used here. At intermediate latitudes ($10° < |b| \leq 30°$), most of the Galactic emission arises from cosmic-ray interactions with neutral material, while at higher latitudes ($> 30°$) the contributions from the ionized medium and the inverse Compton component become important due to the larger scale heights of the ionized gas and the low-energy photons. Since the spatial distribution of the low-energy photon density (near-IR, far-IR, optical, and UV) in the Galaxy is uncertain, the inverse Compton calculation is not well determined. Furthermore, the true cosmic-ray electron scale height is not known. The deconvolution of the observed Galactic radio synchrotron data provides only a lower limit to the cosmic-ray electron scale height of 1 kpc (Broadbent, Haslam, & Osborne 1989) since the Galactic magnetic field distribution is not well understood. Consequently, the current results on the extragalactic background emission are subject to these uncertainties, but recall that this is not the dominant component. Hunter et al. (1997) have shown that there is good agreement between the observed high-energy gamma-ray diffuse radiation in the Galactic plane and the calculations. In the next section, the calculations are compared to observations at all latitudes. The method for treating uncertainties in deriving the extragalactic emission is also discussed.

4. ANALYSIS

The contribution from the 157 sources from the second EGRET source catalog and its supplement (Thompson et al. 1995, 1996), observed in excess of the diffuse background was modeled and subtracted from the data. A new set of binned maps (0.5×0.5 pixels) of event counts and instrument exposure containing only contributions from unresolved sources, Galactic diffuse and extragalactic diffuse radiation, were used for the analysis that follows. Since the determination of the residual, presumably extragalactic radiation, depends critically on the degree to which the calculated Galactic component matches the true Galactic diffuse emission, it is important to demonstrate here the consistency of the predictions with the observations at all latitudes. Figure 2 shows calculated and observed emission profiles in Galactic latitude averaged over 60° bands of Galactic longitude. These results indicate the high-latitude calculations are in good agreement in general with the observed diffuse emission. However, in the inner Galaxy near the Galactic center ($\sim |l| \leq 40°$ and $|b| \leq 30°$) the calculated intensities fall below the observed values. This could arise from interstellar material that is not included in the model or additional contributions from inverse Compton processes arising from unmodeled soft photon distributions or unresolved sources. In addition, the local cosmic-ray density distribution could be nonuniform.

In order to derive the extragalactic emission without being very sensitive to the Galactic model used, the following approach is adopted. As described in § 1, the observed emission at high latitudes is assumed to be made up of a

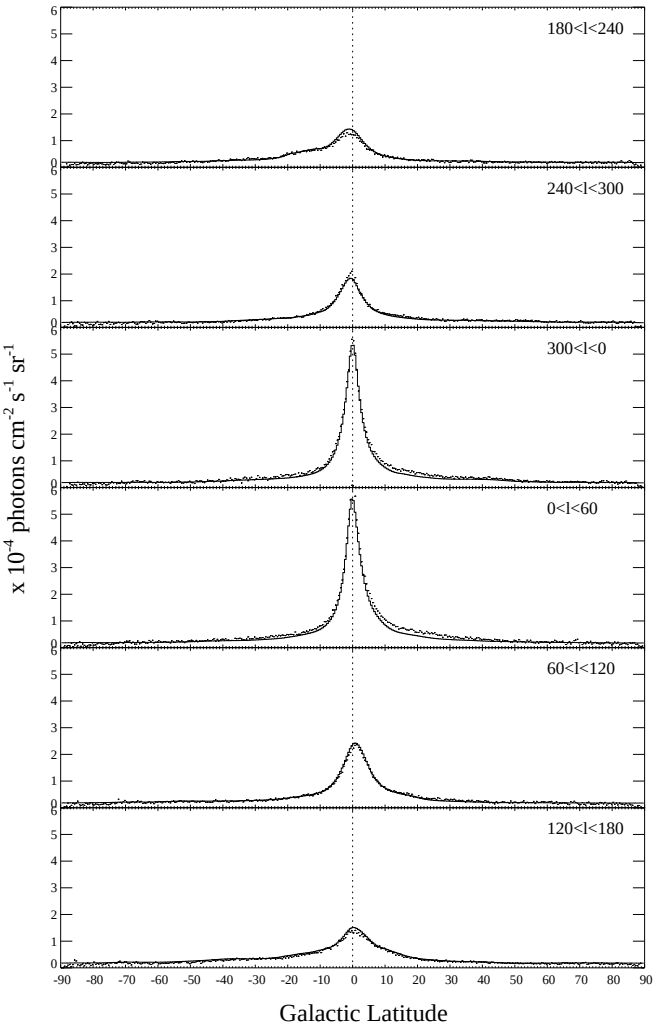

FIG. 2.—Latitude profiles of the observed Galactic emission profile averaged over Galactic longitudes (*data points*). The solid line indicates the calculated values.

Galactic and an extragalactic component. $I_{\rm total}(l, b, E) = A + B \times I_{\rm Gal}(l, b, E)$, where $I_{\rm total}(l, b, E)$ is the total diffuse intensity of high-energy gamma radiation as a function of Galactic coordinates, the gamma-ray energy E, and $I_{\rm Gal}(l, b, E)$ intensity of the Galactic diffuse emission. The slope, B, of a straight line fitted to a plot of observed emission versus the Galactic model gives an independent measure for the normalization of the model while the intercept, A, equals the extragalactic emission. Figure 3 shows the correlation plot for the 10 standard EGRET energy intervals, and Table 1 summarizes the results. The points represent the average intensity within areas of equal solid angle (~ 0.1 sr) covering the whole sky except for an exclusion zone about the Galactic plane ($|b| < 10°$) and the region around the Galactic center ($|l| \leq 40°$ and $10° \leq |b| \leq 30°$). The choice of minimum solid angle bins was made after taking into consideration the limited counting statistics at high and low energies and the distribution of the nonuniform sky coverage. The correlation is not as good at the lowest energy interval of 30–50 MeV and at the highest energy interval (4–10 GeV), primarily due to limited counting statistics. At intermediate energies, the strong correlation provides tight constraints on the normalization of the Galactic diffuse emission. The rather significant deviations in the normal-

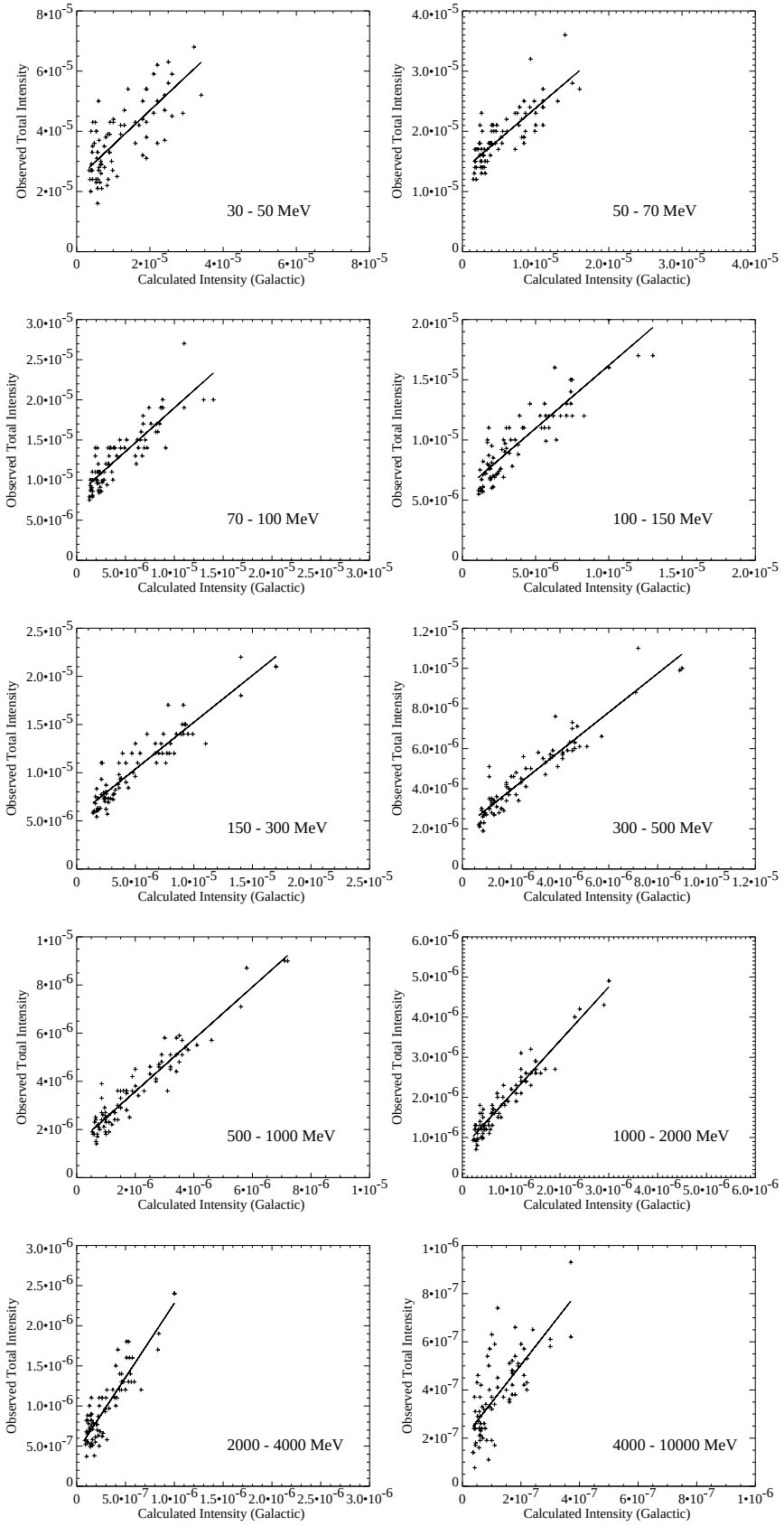

FIG. 3.—Correlation plots of observed diffuse intensity and the calculated Galactic emission. The straight-line fit provides a normalization factor (B) to the calculated Galactic model while the intercept (A) gives the residual emission, independent of the Galactic emission model (see Table 1 for a summary of fit results).

TABLE 1

RESULTS FROM THE ALL-SKY CORRELATION ANALYSIS

Energy (MeV)	Normalization Factor B	A
30–50	1.14	(1.20 ± 0.35)E-06
50–70	1.03	(6.63 ± 1.29)E-07
70–100	1.09	(2.61 ± 0.35)E-07
100–150.....	1.05	(1.10 ± 0.15)E-07
150–300.....	0.97	(3.60 ± 0.48)E-08
300–500.....	0.97	(9.85 ± 1.34)E-09
500–1000	1.09	(2.72 ± 0.37)E-09
1000–2000	1.34	(6.17 ± 0.84)E-10
2000–4000	1.85	(1.52 ± 0.22)E-10
4000–10000.....	1.56	(3.26 ± 0.48)E-11

NOTE.—A is the extragalactic flux in photons cm^{-2} s^{-1} sr^{-1} MeV^{-1}.

ization parameter from unity for energies greater than 1 GeV reflects the spectral discrepancy between the Galactic diffuse model and observations and is discussed in detail by Hunter et al. (1997). This approach yielded the extragalactic gamma-ray spectrum up to 10 GeV. Beyond 10 GeV larger uncertainties exist with the EGRET sensitivity calculation due to the self-veto arising from backsplash in the NaI calorimeter (Thompson et al. 1993). Hence, the results of a Monte Carlo simulation (Y. C. Lin 1992, private communication) are used to determine the differential flux in the 10–30, 30–50, and 50–120 GeV energy ranges. Consequently, these spectral points have additional associated systematic uncertainties. In this analysis, a systematic error of 13% (see Esposito et al. 1997) is assumed for 30–10,000 MeV and 30% beyond 10 GeV. This also takes into account errors in correction factors used to model the changing spark chamber performance with time and photon energy.

In order to examine the isotropy of this emission, the sky was divided into 36 independent regions that excluded the region $|b| < 10°$ at all longitudes, as well as $|l| \leq 40°$ and $10° \leq |b| \leq 30°$ about the Galactic center. The latitude regions near the Galactic center are excluded due to difficulties in accounting for all the Galactic diffuse emission, while the Galactic plane is excluded due to the extreme dominance of the observed emission by the Galactic component. Finally, in deriving the spectrum of the extragalactic emission in each of these regions, it was assumed that the energy-dependent normalization factors for the Galactic calculation (Table 1), derived from the all-sky analysis, remains unchanged for the 36 independent regions of the sky. It would be more appropriate to determine the normalization factors separately in each of the individual regions on the sky; however, statistical limitations give large uncertainties in the results of the correlation analysis.

5. RESULTS

Using the approach described in § 4, the resulting differential photon spectrum of the extragalactic emission averaged over the sky is well fitted by a power law with an index of $-(2.10 \pm 0.03)$. The spectrum was determined using data from 30 MeV to 10 GeV; however, as shown in Figure 4, the differential photon flux in the 10–20 GeV, 20–50 GeV, and 50–120 GeV energy intervals are also consistent with extrapolation of the single power-law spectrum. The integrated flux from 30 to 100 MeV is $(4.26 \pm 0.14) \times 10^{-5}$ photons cm^{-2} s^{-1} sr^{-1}, and that above 100 MeV is $(1.45 \pm 0.05) \times 10^{-5}$ photons cm^{-2} s^{-1} sr^{-1}. These fluxes

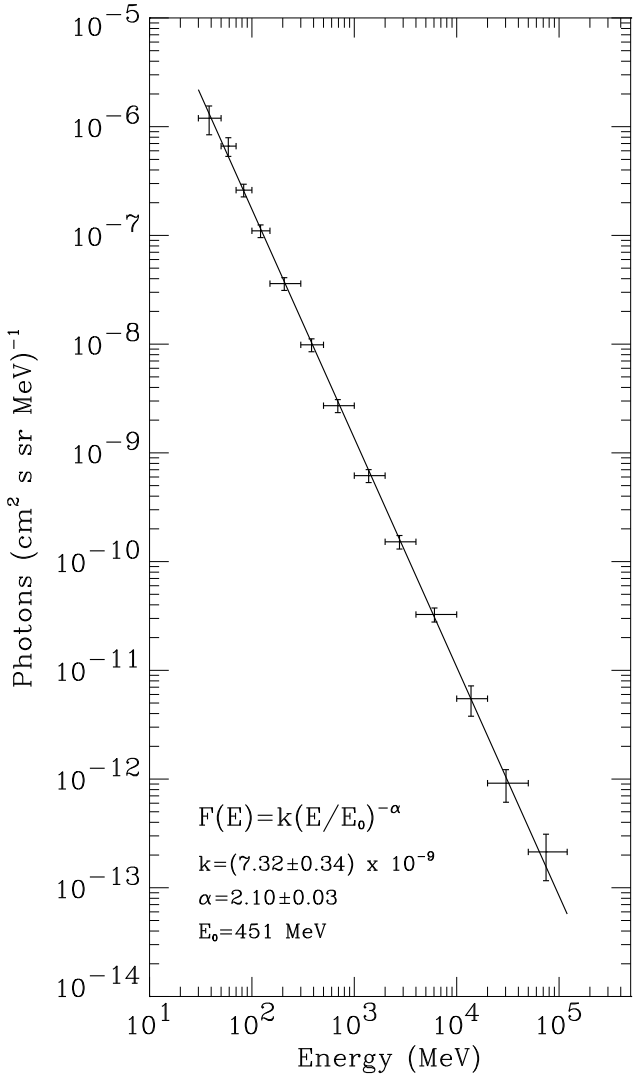

FIG. 4.—The extragalactic diffuse emission spectrum from 30 MeV to 120 GeV.

were determined from the intercept of the straight line fitted to the total observed emission and the Galactic model. This agrees with previously reported *SAS 2* results (Thompson & Fichtel 1982); however, the spectrum is slightly harder.

EGRET observations also permit an examination of the degree of isotropy of the extragalactic emission. The derived integral fluxes in the 36 independent regions of the sky are shown in Figure 5. The flux values range from a low of $(0.89 \pm 0.17) \times 10^{-5}$ photons cm^{-2} s^{-1} sr^{-1} to a high of $(2.28 \pm 0.34) \times 10^{-5}$ photons cm^{-2} s^{-1} sr^{-1}. Figure 6*a* shows a histogram of integral flux values, overlain by a Gaussian fit assuming equal measurement errors. The Gaussian fit yields a mean flux above 100 MeV of 1.47×10^{-5} photons cm^{-2} s^{-1} sr^{-1} with a 1 σ value of 0.33×10^{-5} photons cm^{-2} s^{-1} sr^{-1}, consistent with the all-sky calculation. Of the 36 measurements, 69% fall within 1 σ of the mean, 97% fall within 2 σ, with only the largest value falling outside the 95% confidence interval (Fig. 6*a*). To further examine the spatial distribution, Figures 6*b* and 6*c* show the same data plotted against Galactic longitude and latitude, respectively. No significant deviation from uniformity is observed in the latitude distribution; however, as a function of longitude, there appears to be an enhance-

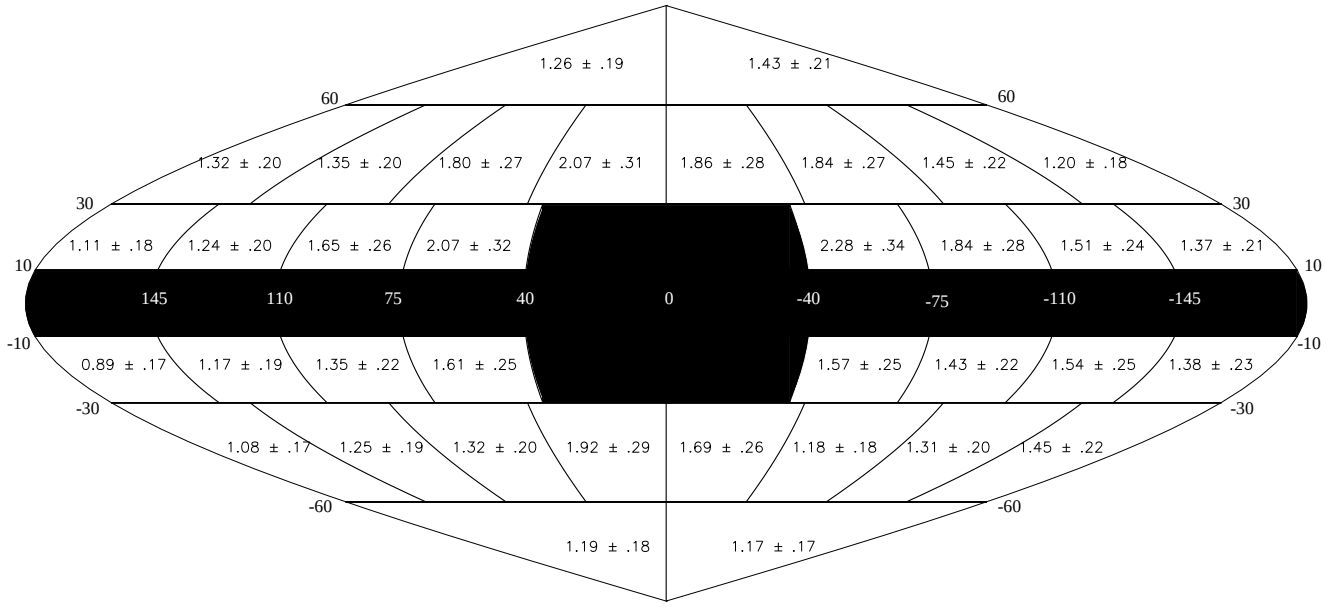

FIG. 5.—The distribution of extragalactic flux ($E > 100$ MeV) in units of 10^{-5} photons cm^{-2} s^{-1} sr^{-1}. The shaded region containing the Galactic plane is excluded due to extreme dominance of the Galactic emission, and the region centered on the Galactic center and extending toward $\pm 30°$ in latitude is excluded due to difficulties in modeling all of the Galactic emission.

ment in the derived intensities toward $\sim l = 20°$, but a closer examination shows this feature to be due to a few regions on the boundary of the excluded Galactic center region. This could arise from unaccounted Galactic diffuse emission. If one excludes the inner regions of the Galaxy ($|r| < 60°$, where r is the angle made with the direction of the Galactic center), the mean flux is 1.36×10^{-5} photons cm^{-2} s^{-1} sr^{-1} above 100 MeV. The distribution of the 28 independent observations is consistent with isotropy (reduced $\chi^2 = 1.09$). As discussed below, the inclusion of additional Galactic emission in the inner Galaxy measurements is not inconsistent with the observed distribution of spectral indices. However, the exact nature of the excess emission in the inner Galaxy is not resolved by this analysis.

Figure 7 shows the distribution of spectral index in 36 independent regions of the sky. The power-law indices vary from $-(2.04 \pm 0.08)$ to $-(2.20 \pm 0.07)$ and show no systematic deviations from the value of $-(2.10 \pm 0.03)$, derived from the all-sky analysis. The histogram of spectral indices shown in Figure 8*a* yields a mean value of -2.11 with a 1 σ value of 0.04. The corresponding longitude and latitude distributions (Figs. 8*b* and 8*c*) show no indication of a smooth variation in the index. The expected distribution of the spectral indices can be calculated if one assumes that the outer Galaxy average represents a better measure of the isotropic extragalactic emission and that the "excess" emission near the Galactic center region arises solely from unaccounted Galactic diffuse emission. The expected distribution should be characterized by an average of -2.12 with a standard deviation of 0.04. This is consistent with the average value of $-(2.11 \pm 0.04)$ derived from the all-sky distribution shown in Figure 7. Finally, a distribution of the integral flux above 100 MeV versus the corresponding spectral index is shown in Figure 9. Even though the Galactic diffuse emission spectrum is not well characterized by a single power law (Hunter et al. 1997), such a characterization in the 30–10,000 MeV energy range would in general yield a harder spectral index ($\sim$1.8–1.9) than that of the derived extragalactic emission. Hence, any significant Galactic contribution to the derived extragalactic emission would show evidence for some correlation between the integral flux and the spectrum. With the exception of a few points with the highest intensity, there is no correlation between the intensity and the spectral index. As stated before, these high points by themselves only suggest the presence of a small residual Galactic component in some of the inner Galaxy measurements.

6. DISCUSSION

The results just presented have confirmed the existence of a generally uniform, presumably extragalactic diffuse radiation, consistent in intensity with that determined by the *SAS 2* experiment. They are generally consistent with the preliminary results from Sreekumar & Kniffen (1996), Kniffen et al. (1996), Osborne, Wolfendale, & Zhang (1994), and Chen, Dwyer, & Kaaret (1996) that were all based on a smaller set of observational data. The presence of significant excess emission from ($l \sim 90°$, $b \sim 52°$) to ($l \sim 45°$, $b \sim 77°$) reported by Chen et al. (1995) is not as evident in our analysis, possibly due to the more stringent zenith angle selection. Osborne, Wolfendale, & Zhang (1994) obtained a smaller integral flux, probably a result of attributing a larger contribution from the inverse Compton process to the Galactic diffuse emission. The results presented here, which were obtained using a larger data set and a much more careful accounting of other contributing effects, have greatly extended the energy spectral information both in precision and energy range, as well as provided substantial additional information on its uniformity. Combined with the X-ray and low-energy gamma-ray information, a spectrum for the uniform diffuse radiation now exists over a broad energy range (Fig. 10).

A large number of possible origins for the extragalactic diffuse gamma-ray emission have been proposed over the years. Fichtel & Trombka (1981) have reviewed some of the proposed models.

Theories of diffuse origin include scenarios of baryon

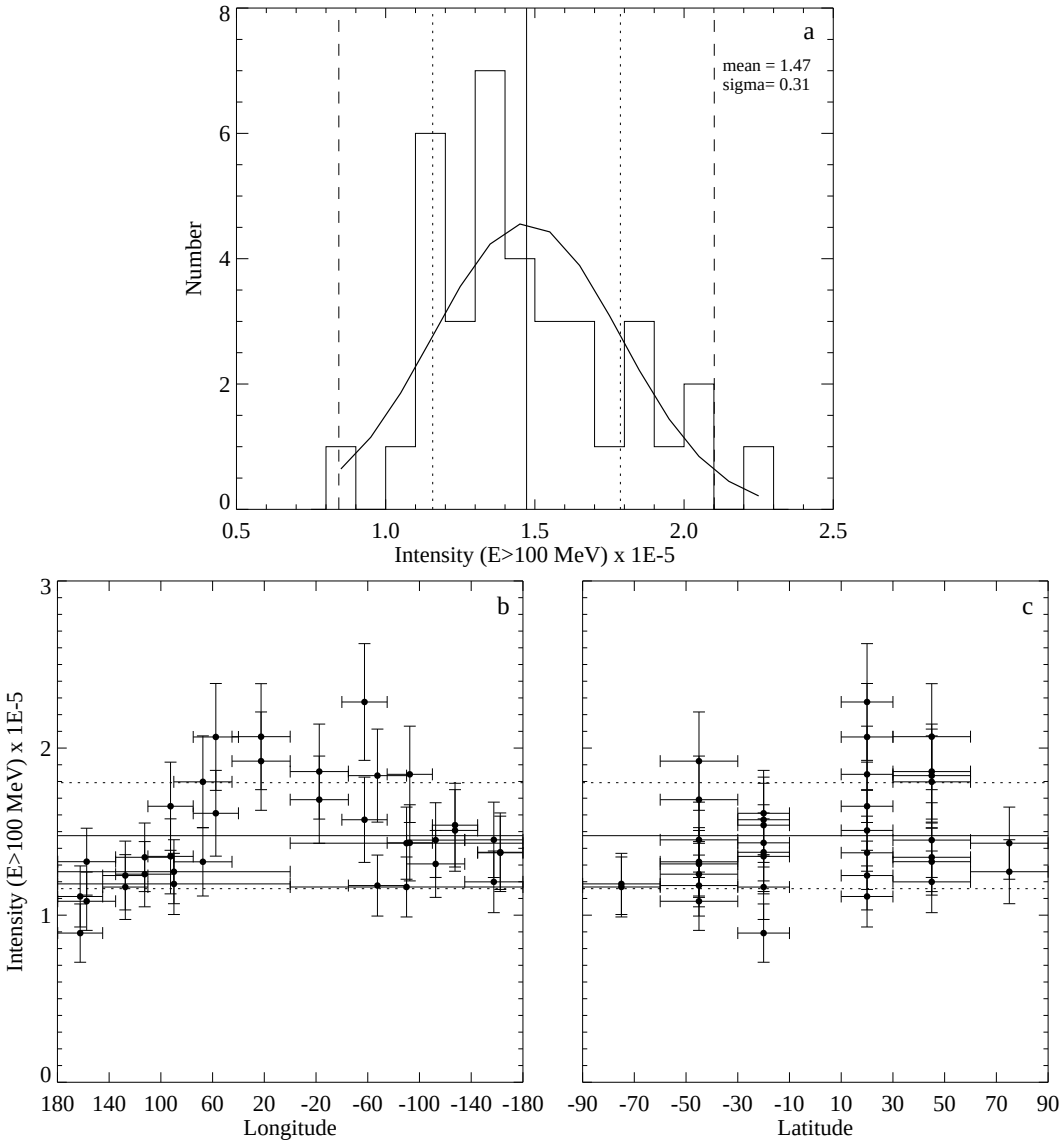

FIG. 6.—The all-sky distribution of integral flux ($E > 100$ MeV) in units of photons cm^{-2} s^{-1} sr^{-1}. (*a*) Gaussian fit to the flux histogram showing the mean (*solid line*), 1 σ (*dotted line*), and 2 σ (*dashed line*) confidence intervals. (*b*) and (*c*) Intensity values plotted over longitude and latitude, respectively. The longitude distribution shows slightly larger intensity values within $\pm 60°$ (see discussion in § 5).

symmetric universe (Stecker, Morgan, & Bredekamp 1971), primordial black hole evaporation (Page & Hawking 1976; Hawking 1977), million solar mass black holes that collapsed at high redshift ($z \sim 100$) (Gnedin & Ostriker 1992), and some exotic source proposals, such as annihilation of supersymmetric particles (Silk & Srednicki 1984; Rudaz & Stecker 1991; Kamionkowski 1995). All of these theories predict continuum or line contributions that are unobservable above 30 MeV with current instruments.

Models based on discrete source contributions have considered a variety of source classes. Normal galaxies might at first appear to be a reasonable possibility for the origin of the diffuse radiation since they are known to emit gamma rays and to do so to very high gamma-ray energies (Sreekumar et al. 1992; Hunter et al. 1997). Previous estimates (Kraushaar et al. 1972; Strong, Wolfendale, & Worrall 1976; Lichti, Bignami, & Paul 1978; Fichtel et al. 1978) have shown that the intensity above 100 MeV expected from normal galaxies is only about 3%–10% of what is observed. Further and perhaps even more significant, the energy spectrum of the Galactic diffuse gamma rays is significantly different from that measured by EGRET for the extragalactic diffuse radiation, as it is harder at low energies (100 to 1000 MeV) and considerably steeper in the 1 to 50 GeV region. Dar & Shaviv (1995) have suggested that emission arises from cosmic-ray interaction with intergalactic gas in groups and clusters of galaxies. Although the authors claim that this proposed explanation leads to a higher intensity level, it is still in marked disagreement with the measured energy spectrum (Stecker & Salamon 1996a). Clearly, small contributions from a number of these proposed sources remains viable. A fluctuation analysis (Willis 1996) indicates that $\sim 10\%$ to 100% of the emission could be made up of unresolved point sources and does not very well constrain the likely contribution from a diffuse origin.

It has been postulated for over 2 decades by a large number of authors that active galaxies might be the source

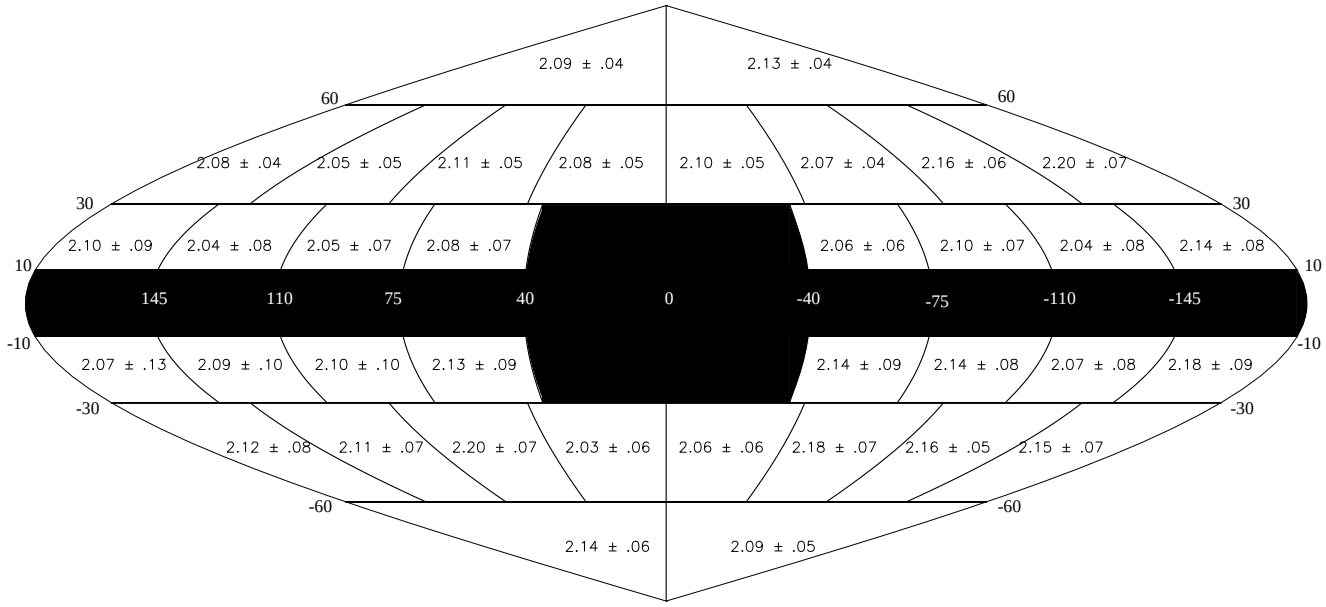

FIG. 7.—The distribution of power-law spectral indices

of this general high-energy gamma-ray diffuse emission (e.g., Bignami et al. 1979; Kazanas & Protheroe 1983). However, prior to the results from EGRET, only one quasar had been seen in high-energy gamma rays (3C 273), so there was little data upon which to base a calculation of the expected intensity. Now, a large number of high-energy gamma-ray–emitting blazars have been observed by EGRET (von Montigny et al. 1995; Mukherjee et al. 1997). One of the more important pieces of evidence in favor of the blazar origin of the high- energy portion of the diffuse spectrum is the spectrum. Both the spectrum reported here and the average spectrum of blazars may be well represented by a power law in photon energy. The spectral index determined here for the diffuse radiation is $-(2.10 \pm 0.03)$, and the average spectral index of the observed blazars is $-(2.15 \pm 0.04)$. These two numbers are clearly in good agreement. A standard cosmological integration of a power law in energy yields the same functional form and slope. Considering the new, well-determined gamma-ray spectrum, this argues strongly that the bulk of the observed extragalactic gamma-ray emission can be explained as originating from unresolved blazars.

In order to estimate the intensity of the diffuse radiation from blazars, knowledge of the evolution function is needed, as well as the intensity distribution of the blazars. Two approaches have been utilized to determine the gamma-ray evolution. One way is to assume that the evolution is similar to that at other wavelengths. The other alternative is to deduce the evolution from the gamma-ray data itself and hence have a solution that depends only on the gamma-ray results. The advantage of the former is that if the assumption of a common evolution is correct, an estimate with less uncertainty is obtained. The positive aspect of the latter is that there is no assumption of this kind, but the uncertainty in the calculated results is relatively large because of the small gamma-ray blazar sample.

Several authors have estimated the contribution from blazars using the first approach described above (Padovani et al. 1993; Stecker, Salamon, & Malkan 1993; Setti & Woltjer 1994; Erlykin & Wolfendale 1995; Stecker & Salamon 1996b), where one accepts the proposition that the evolution function determined from the radio data may be applied to the gamma-ray–emitting blazars. The recent work of Mukherjee et al. (1997) shows that there is agreement within uncertainties between the radio and high-energy gamma-ray z distributions of both types of blazars, i.e., flat-spectrum radio quasars and BL Lac objects. The calculations agree with the observation of the intensity of the diffuse radiation, with the uncertainty varying with the approach and estimated errors. In most cases, the calculations are within 50% of the observed spectrum. A word of caution seems appropriate, since it should be pointed out that the degree and nature of the correlation between the radio and gamma-ray emission is still being debated (Padovani et al. 1993; Mücke et al. 1996; Mattox et al. 1997). The calculations of Stecker & Salamon (1996b) predict a curvature in the blazar background spectrum; our data, while being well represented by a single power law, do not rule out such a curvature, at least up to few GeV.

Chiang et al. (1995) used only the gamma-ray blazar data to deduce the evolution function for the gamma-ray–emitting blazars. They used the $V/V_{\max}$ approach in the context of pure luminosity evolution (currently the preferred concept) to show that there was indeed evolution of the high-energy gamma-ray–emitting blazars and to deduce the parameters describing the evolution. These authors found that the evolution was consistent within errors to that seen at other wavelengths. Their estimated intensity level ranges from $(1.9^{+8.5}_{-1.4}$ to $2.6^{+11.4}_{-1.8}) \times 10^{-5}$ photons cm^{-2} s^{-1} sr^{-1} for $E > 100$ MeV, which indicates large uncertainties due to the unconstrained nature of the lower end of the luminosity function.

With regard to the isotropy, as described earlier, the data in the region $\sim 60°$ away from the Galactic center show no detectable deviation from isotropy within the limits of the EGRET measurements. The slight enhancement in the derived extragalactic intensity toward the Galactic center is believed to arise mostly from additional Galactic inverse

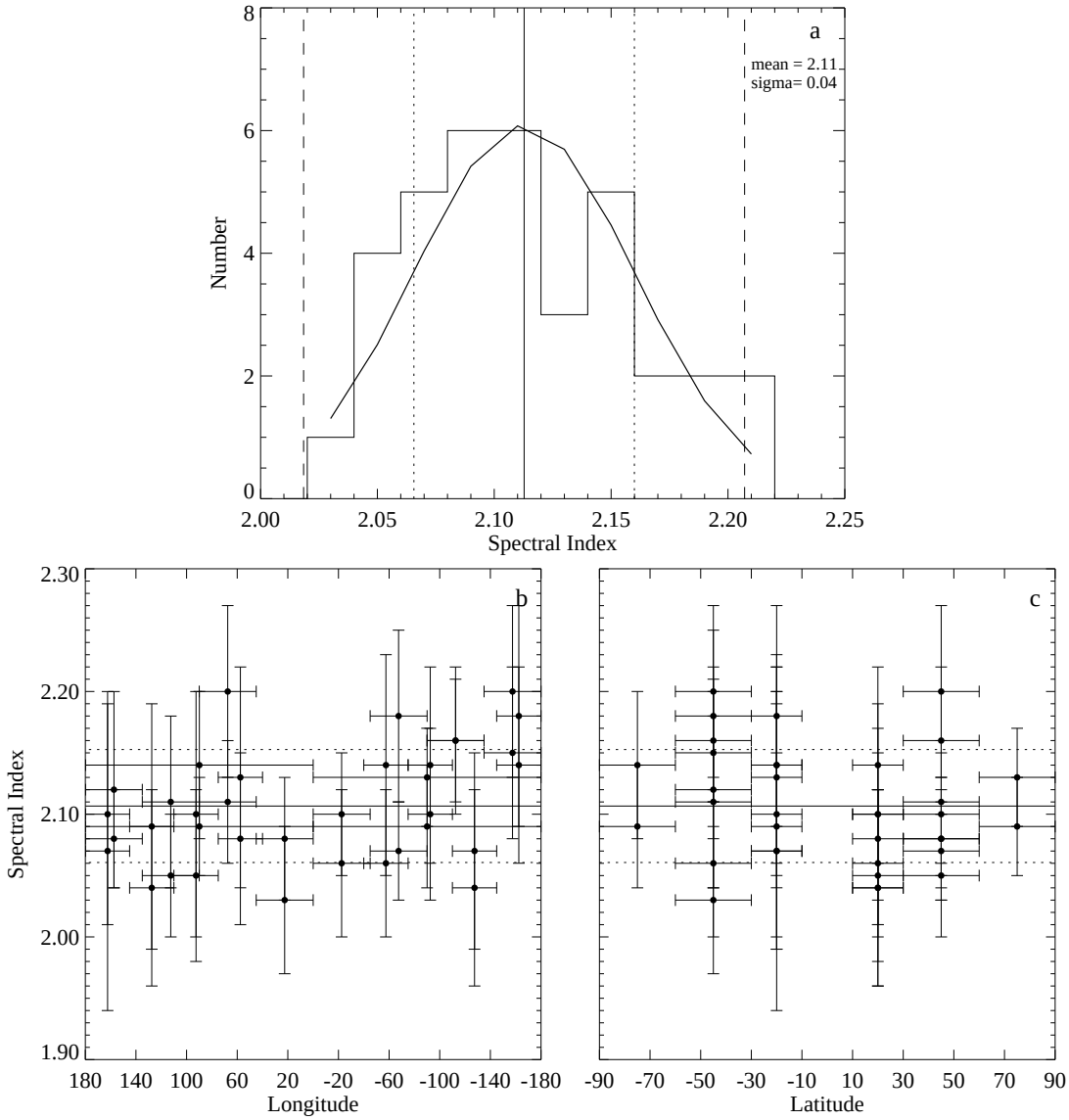

FIG. 8.—The all-sky distribution of the power-law spectral index. (*a*) Gaussian fit to the spectral index histogram showing the mean (*solid line*), 1 σ (*dotted line*), and 2 σ (*dashed line*) confidence intervals. (*b*) and (*c*) Spectral index values plotted over longitude and latitude, respectively, showing the absence of any variation over the sky.

Compton contribution that has not been modeled due to large intrinsic uncertainties in the soft photon distribution. No evidence for any smooth angular variation is present in the power-law spectrum used to characterize the extragalactic emission.

In examining the extragalactic diffuse spectrum from the X-ray to gamma-ray spectral region, it has been suggested (Zdziarski 1996) that the combination of Seyfert I and Seyfert II, and a likely contribution from supernovae (The, Leising, & Clayton 1993), appears sufficient to explain the observed radiation from 1 keV to a few mega–electron volts. Although at this point in time, both the observational and theoretical picture of the extragalactic gamma-ray emission below 10 MeV is unclear, it appears that at higher energies, EGRET observations discussed in this paper strongly suggest that the predominant origin of the gamma radiation in the region from 30 MeV to at least 50 GeV is blazar emission. Other explanations for this high-energy gamma-ray region seem to be inconsistent with at least one aspect of the observations, with the well-measured high-energy gamma-ray spectrum being a particularly strong discriminator.

If the hypothesis that the general diffuse radiation is the sum of the emission of blazars is accepted, there is an interesting corollary. The spectrum of the measured extragalactic emission implies the average quiescent energy spectra of blazars extend to at least 50 GeV and maybe up to 100 GeV without a significant change in slope. Most of the measured spectra of individual blazars only extend to several GeV and none extend above 10 GeV, simply because the intensity is too weak to have a significant number of photons to measure. Intergalactic absorption does not have much effect at this energy except for blazars at relatively large z, and, in any case would have a depressing effect on the spectrum. Hence, the continuation of the single power-law diffuse spectrum up to 100 GeV really implies that the source spectrum also continues without a major change in spectral slope to at least 100 GeV. This

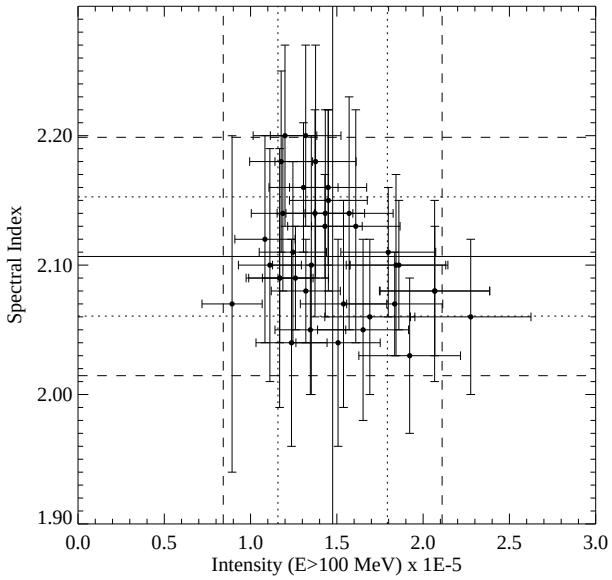

FIG. 9.—Integrated intensities ($E > 100$ MeV), plotted against the derived power-law spectral indices for different regions of the sky, indicate no evidence for any correlation.

conclusion, in turn, implies that the spectrum of the parent relativistic particles in blazars that produce the gamma rays remains hard to even higher energies.

The authors wish thank Andrzej Zdziarski for providing the results of the various model calculations in machine readable form and Betty Rots for valuable editorial comments. The EGRET team gratefully acknowledges support from the following: Bundesministerium für Bildung, Wissenschaft, Forschung und Technologie grant 50 QV 9095 (MPE), NASA Cooperative Agreement NCC 5-95 (HSC), NASA grant NAG5-1605 (SU), and NASA contract NAS5-96051 (NGC).

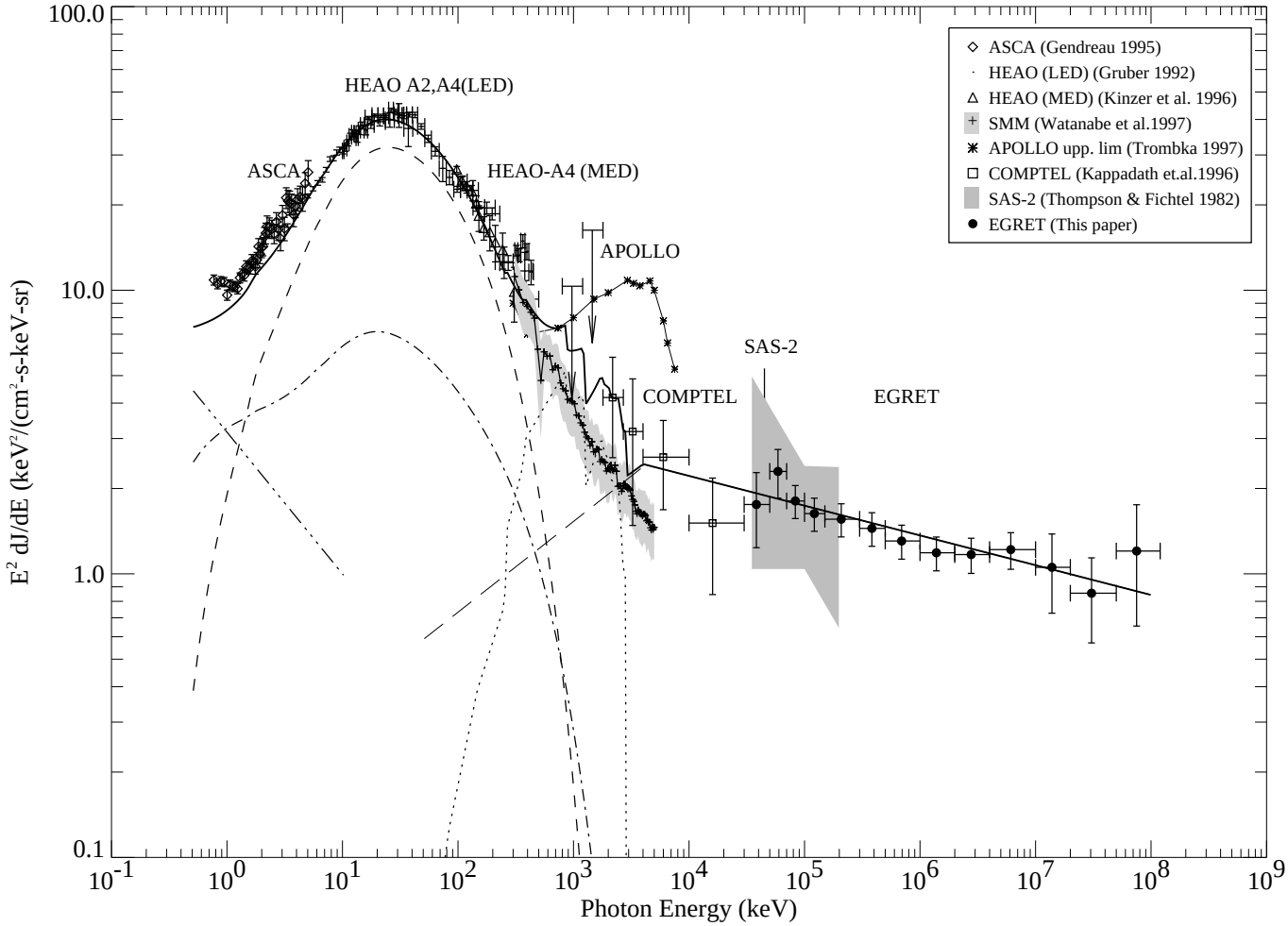

FIG. 10.—Multiwavelength spectrum of the extragalactic gamma-ray spectrum from X-rays to high-energy gamma rays. The estimated contribution from Seyfert I (*dot-dashed line*), and Seyfert II (*dashed*) are from the model of Zdziarski (1996); steep-spectrum quasar contribution (*triple-dot–dashed line*) is taken from Chen, Fabian, & Gendreau (1997); Type Ia supernovae (*dotted line*) is from The et al. (1993). The blazar contribution below 4 MeV (*long-dashed line*) is derived assuming the average blazar spectrum breaks around 4 MeV (McNaron-Brown et al. 1995) to a power law with an index of ~ -1.7. The thick solid line indicates the sum of all the components.

REFERENCES

Bailes, M., & Kniffen, D. A. 1992, ApJ, 391, 659
Bertsch, D. L., Dame, T. M., Fichtel, C. E., Hunter, S. D., Sreekumar, P., Stacy, J. G., & Thaddeus, P. 1993, ApJ, 416, 587
Bignami, G. F., Fichtel, C. E., Hartman, R. C., & Thompson, D. J. 1979, ApJ, 232, 649
Broadbent, A., Haslam, C. G. T., & Osborne, J. L. 1989, MNRAS, 237, 381
Chen, A., Dwyer, J., & Kaaret, P. 1995, ApJ, 445, L109
———. 1996, ApJ, 463, 169
Chen, L. W., Fabian, A. C., & Gendreau, K. C. 1997, MNRAS, 285, 449
Chiang, J., Fichtel, C. E., von Montigny, C., Nolan, P. L., & Petrosian, V. 1995, ApJ, 452, 156
Comastri, A., Setti, G., Zamorani, G., & Hasinger, G. 1995, A&A, 296, 1
Dame, T. M., et al. 1987, ApJ, 322, 706
Dar, A., & Shaviv, N. 1995, Phys. Rev. Lett., 75, 3052
Derdeyn, S. M., Ehrmann, C. H., Fichtel, C. E., Kniffen, D. A., & Ross, R. W. 1972, Nucl. Instrum. Methods Phys. Rev., 98, 557
Dickey, J. M., & Lockman, F. J. 1990, ARA&A, 28, 215
Erlykin, A. D., & Wolfendale, A. W. 1995, J. Phys. G, 21, 1149
Esposito, J. A., et al. 1997, ApJ, submitted
Fichtel, C. E., et al. 1975, ApJ, 198, 163
Fichtel, C. E., et al. 1977, ApJ, 217, L9
———. 1993, AIP Conf. Proc. 2, Compton Symposium, ed. C. E. Fichtel, N. Gehrels, & J. P. Norris (New York: AIP), 304, 721
Fichtel, C. E., Simpson, G. A., & Thompson, D. J. 1978, ApJ, 222, 833
Fichtel, C. E., & Trombka, J. I. 1981, Gamma-Ray Astrophysics, New Insights into the Universe, NASA SP-453 (Washington: GPO)
Gendreau, K. C. 1995, Ph.D. thesis, Massachussets Institute of Technology
Gnedin, N. Y., & Ostriker, J. P. 1992, ApJ, 400, 1
Gruber, D. E. 1992, The X-Ray Background, ed. X. Barcons & A. C. Fabian (Cambridge: Cambridge Univ. Press), 44
Hawking, S. W. 1977, Scientific American, 236, 34
Hunter, S. D., et al. 1997, ApJ, 481, 205
Kamionkowski, M. 1995, The Gamma Ray Sky with Compton *GRO* and SIGMA, ed. M. Signore, P. Salati, & G. Vedrenne (Dordrecht: Kluwer), 113
Kanbach, G., et al. 1988, Space Sci. Rev., 49, 69
Kappadath, S. C., et al. 1996, A&AS, 120, 619
Kazanas, D., & Protheroe, J. P. 1983, Nature, 302, 228
Kinzer, R. L., Jung, G. V., Gruber, D. E., Matteson, J. L., & Peterson, L. E. 1997, ApJ, 475, 361
Kniffen, D. A., et al. 1996, A&AS, 120, 615
Kraushaar, W. L., et al. 1972, ApJ, 177, 341
Leiter, D., & Boldt, E. 1992, in AIP Conf. Proc. 254, Testing the AGN Paradigm (New York: AIP), 370
Lichti, G. G., Bignami, G. F., & Paul, J. A. 1978, Ap&SS, 56, 403
Mattox, J. R., Schachter, J., Molnar, L., Hartman, R. C., & Patnaik, A. R. 1997, ApJ, 481, 95.
McNaron-Brown, K., et al. 1995, ApJ, 451, 575
Mücke, A., Pohl, M., Reich, P., Reich, W., Schlickeiser, R., & Kanbach, G. 1996, A&AS, 120, 541
Mukherjee, R., et al. 1997, ApJ, 490, 116
Osborne, J. L., Wolfendale, A. W., & Zhang, L. 1994, J. Phys. G., 20, 1089
Padovani, P., Ghisellini, G., Fabian, A. C., & Celotti, A. 1993, MNRAS, 260, L21
Page, D. N., & Hawking, S. W. 1976, ApJ, 206, 1
Rudaz, S., & Stecker, F. W. 1991, ApJ, 368, 40
Setti, G., & Woltjer, L. 1994, ApJS, 92, 629
Silk, J., & Srednicki, M. 1984, PRL, 53, 624
Sreekumar, P., & Kniffen, D. A. 1996, in IAU Symp. 168, Examining the Big Bang and Diffuse Background Radiations, ed. M. Kafatos & Y. Kondo (Dordrecht: Kluwer), 279
Sreekumar, P. et al. 1992, ApJ, 400, L67
Stecker, F. W., Morgan, D. L., & Bredekamp, J. 1971, PRL, 27, 1469.
Stecker, F. W., & Salamon, M. H. 1996a, Phys. Rev. Lett., 76, 3878
———. 1996b, ApJ, 464, 600
Stecker, F. W., Salamon, M. H., & Malkan, M. 1993, ApJ 410, L71
Strong, A. W., Wolfendale, A. W., & Worrall, D. M. 1976, J. Phys. A, 9, 1553
Taylor, J., & Cordes, J. 1993, ApJ, 411, 674
The, L.-S., Leising, M. D., & Clayton, D. D. 1993, ApJ, 403, 32
Thompson, D. J., Simpson, G. A., & Özel, M. E. 1981, J. Geophys. Res., 86, 1265
Thompson, D. J., & Fichtel, C. E. 1982, A&A, 109, 352
Thompson, D. J., et al. 1993, ApJS, 86, 629
———. 1995, ApJS, 101, 259
———. 1996, ApJS, 107, 227
von Montigny, C., et al. 1995, ApJ, 440, 525
Watanabe, K., et al. 1997, in AIP Conf. Proc. 410, Fourth Compton Symposium, ed. C. D. Dermer, M. S. Strickman, & J. D. Kurfess (New York: AIP), in press
Willis, T. D. 1996, Ph.D. thesis, Stanford Univ.
Zdziarski, A. A. 1996, MNRAS, 281, L9
Zdziarski, A. A., Johnson, N. W., Done, C., Smith, D., & McNaron-Brown, K. 1995, ApJ, 438, L63